# Capturing Carbon Dioxide from Power Plant Flue Gas Using One-Stage and Two-Stage Pressure Swing Adsorption Technology

Chemistry and Environmental Research Lab: Chuang, Tsung-Yu; Shen, Wei-Chen; Kao, Ching-Di; Huang, Hsiao-Yu; Tu, Si-Hong

## 1. Introduction

In recent years, the concentration of carbon dioxide in the atmosphere has been rising gradually. In NOAA's report of February 2024, the global average atmospheric CO2 level has reached 421.40 ppm. On April 21st of the 111th year [Taiwanese calendar], the country passed a revision of the "Greenhouse Gas Reduction and Management Act" to the "Climate Change Response Act" and requested the Legislative Yuan's review. At the same time, the national long-term carbon reduction target was revised to "net-zero emissions by 2050," reinforcing the country's regulatory strength over greenhouse gas emissions. This study begins with the confirmation of the effectiveness of solid $CO_2$ adsorbents in the laboratory, using 13X as the solid adsorbent, and based on this, establishes the VPSA (Vacuum Pressure Swing Adsorption) one-stage and two-stage $CO_2$ separation processes, which mainly include high-pressure adsorption, co-current depressurization, pressure equalization, vacuum desorption, and stand-by processes, attempting to capture $CO_2$ in a low-energy, solvent-free, and low-desorption-energy manner.

## 2. Experimental Results

Initially, the isothermal equilibrium adsorption curve experiments (as shown in Figure 1.) were conducted to determine the Langmuir parameters, which allow for the calculation of operable carbon dioxide during adsorption and desorption. Under conditions of 3.0 bar adsorption pressure and 0.1 bar desorption pressure, the operable amount of $CO_2$ is the difference between the adsorption at 3.0 bar and 0.1 bar. It estimates the total amount of $CO_2$ that can be separated in a complete adsorption-desorption cycle. Figure 2. confirms that 13X has the highest operability at 25 ℃, separating approximately 3.38 mol $CO_2$ per kilogram of adsorbent. Although the separation capacity drops to about 2.90 mol $CO_2$ per kilogram of adsorbent at 70 ℃, it maintains over 80% of its operability.

The adsorbent is regenerated at a temperature of 250 ℃ to remove the water before its first use. In practice, high-temperature regeneration is not performed every time; thus, a simple regeneration at 30 ℃ simulating field conditions was conducted in the laboratory. Subsequent isothermal adsorption curve experiments were performed to obtain Langmuir parameters. Assuming the initial Qm (maximum adsorption capacity) to be 100%, the subsequent decay of Qm is shown in Figure 3. The second Qm is only 83.71% of the first, indicating a certain degree of decline. However, the fifth Qm retains 81.65% of the first, with subsequent decay only 2% or less. Consequently, it can be estimated that the subsequent separation operability per kilogram of adsorbent at 25 ℃ and 70 ℃ should be above 2.76 and 2.470 mol $CO_2$, respectively.

Long-term carbon dioxide separation experiments using a three-bed nine-step process with actual flue gas were conducted, with the main equipment shown in Figures 4. and 5., and the schematic diagram depicted in Figure 6. Results for

each cycle are presented in Figure 7. The $CO_2$ concentration of the feed gas was approximately 12.19±0.98%, with an adsorption pressure of about 3.0±0.22 bar and a vacuum desorption pressure of around 0.12±0.10 bar. Pressure balance during depressurization and pressurization was approximately 1.62±0.14 bar and 1.30±0.08 bar, respectively. After separation, the average concentration of $CO_2$ was 91.45±3.37%, and after long-term operation, the average concentration for the last ten cycles was 90.74±1.25%, confirming the stability of $CO_2$ separation with this process.

The schematic diagram of the two-stage CO2 separation process is shown in Figure 8. The $CO_2$ concentration of the feed gas for the first stage of the two-bed six-step experiment was 12.61±0.27%, with an average post-separation concentration of 83.41±0.94%. The average concentration for the last ten cycles was 84.02±0.25% (results for each cycle in the first stage are shown in Figure 9.). The feed gas $CO_2$ concentration for the second stage single-bed three-step was 82.98±1.30%, with an average post-separation concentration of 88.93±1.86%. The average concentration for the last ten cycles was 88.44±0.90% (results for each cycle in the second stage are shown in Figure 10.), confirming the stable separation of $CO_2$ in both stages.

The VPSA process uses flue gas treated for acid and water removal. In the one-stage $CO_2$ separation process of this study, the average concentration of $CO_2$ in the feed was 12.19±0.98%, with a final $CO_2$ concentration after separation reaching 90.74±1.25%. For the two-stage $CO_2$ separation process, the feed had an average $CO_2$ concentration of 12.61±0.27%, with a final concentration of about 88.44±0.90%, but the recovery rate was 52.89±3.72%, which was higher than the first stage. This research has confirmed that the one-stage and two-stage processes can stably and continuously separate $CO_2$ from flue gases over long periods, each having its operational focus.

Regarding energy consumption, approximately 65~78% of the total process energy is concentrated on the dual-bed, non-thermal desiccant dryers. The energy requirements for the one-stage and two-stage VPSA processes are approximately 1.72±0.10 and 2.53±0.12 GJ/ton $CO_2$, respectively (as shown in Figure 11.). The energy consumption is higher for the two-stage process due to additional control equipment, but this increase of 0.81±0.15 GJ/ton $CO_2$ in energy consumption significantly enhances the recovery rate by 52.89±3.72%. Therefore, the one-stage and two-stage operational strategies can be chosen based on site requirements for a high recovery rate or purity, enhancing application flexibility in process sites.

## 3. Future

This analysis indicates that the CO2 concentration of the feed greatly influences the CO2 concentration of the product after separation. About 1~2% variation in the feed can affect the product concentration by 5.35-6.56%. Therefore, future designs of the two-stage process should focus on high recovery rates in the first stage and high concentration in the second stage to maximize $CO_2$ capture efficiency.

Since most of the energy consumption is concentrated in the dehydration part, subsequent energy improvements could aim at reducing dehydration. Experiments could be planned to integrate the heat released during adsorption and the heat absorbed during desorption, conducting quasi-thermal integration tests. Moreover, by incorporating

the concept of human factors engineering, the convenience and safety of adsorbent replacement can be enhanced, reducing the hazards associated with experimentation. The feasibility of scaling up for further experiments can be assessed depending on the maturity of the process development.

## 4. Figures

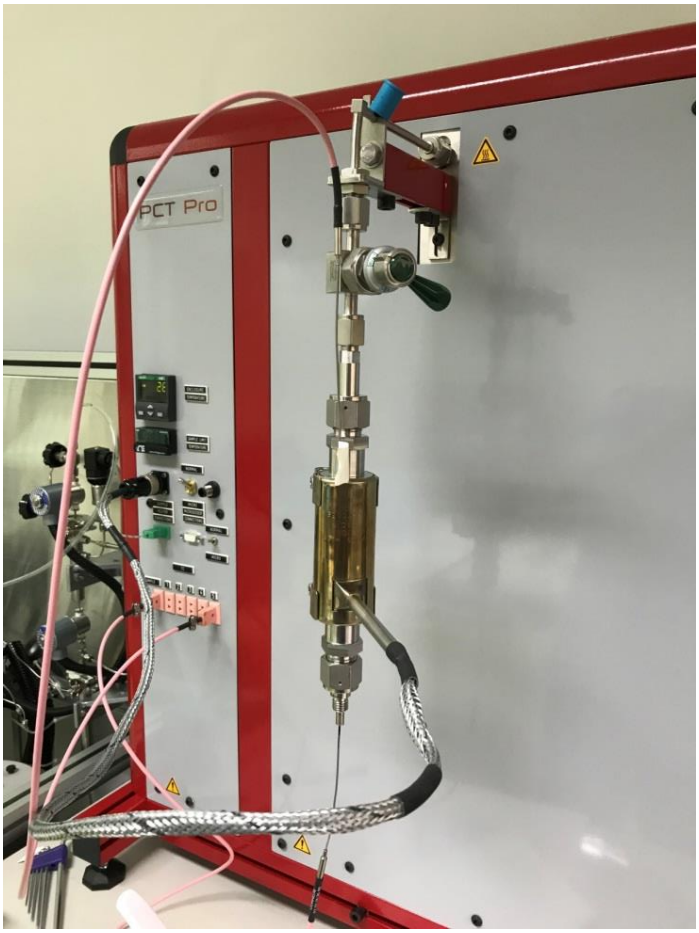


Figure 1: Equipment for Measuring the $CO_2$ Adsorption Efficiency of Solid Adsorbents (Photographed by TPRI)

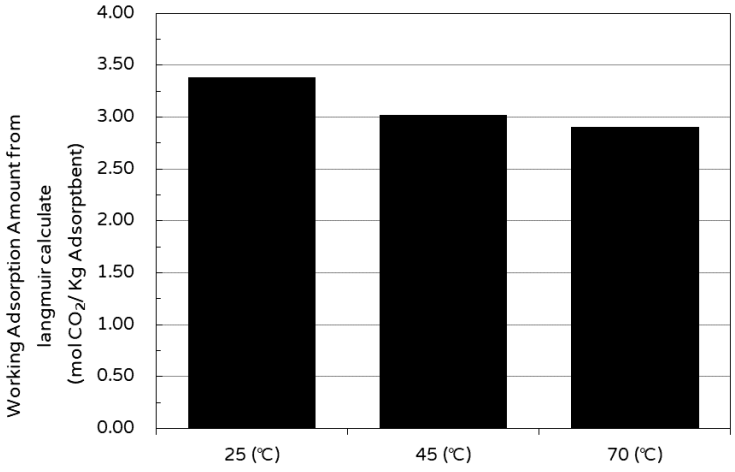


Figure 2: Operable $CO_2$ Adsorption Capacity Calculated by the Langmuir Model from 0.1 bar to 3.0 bar (Graphed in Excel by TPRI)

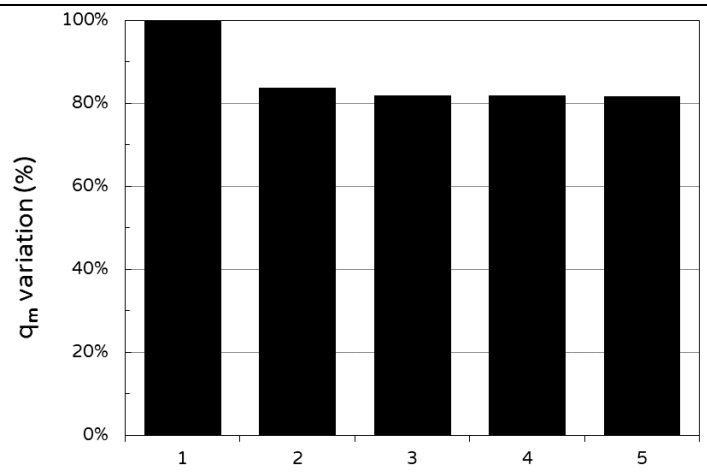


Figure 3: Decay Variation of Qm with Repeated Use of 13X (Graphed in Excel by TPRI)


Figure 4: Container Equipment of VPSA (Two 20-foot Yellow and Blue Containers) (Photographed by TPRI)

Figure 5: Three-Bed Pressure Swing Adsorption Main Equipment (Photographed by TPRI)

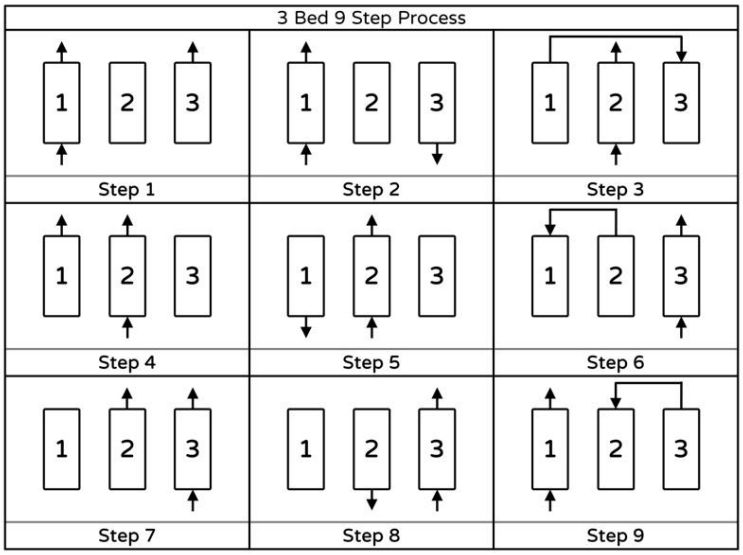


Figure 6: Schematic Diagram of the VPSA One-Stage Three-Bed Nine-Step Operation Process (Graphed in PowerPoint by TPRI)

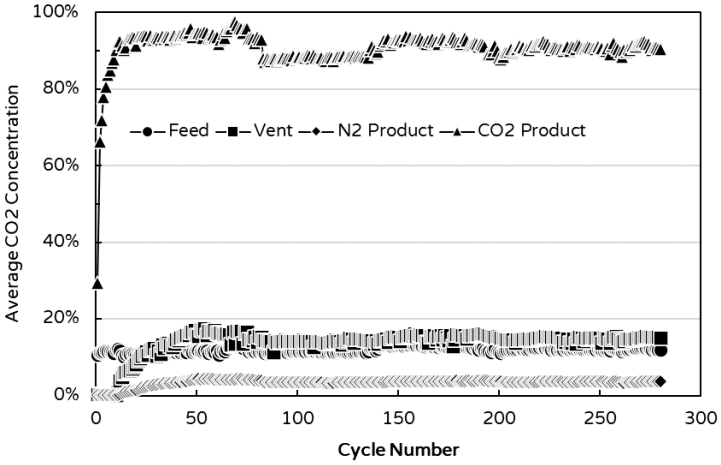


Figure 7: Average $CO_2$ Concentration for Each Cycle in VPSA One-Stage (Graphed in Excel by TPRI)

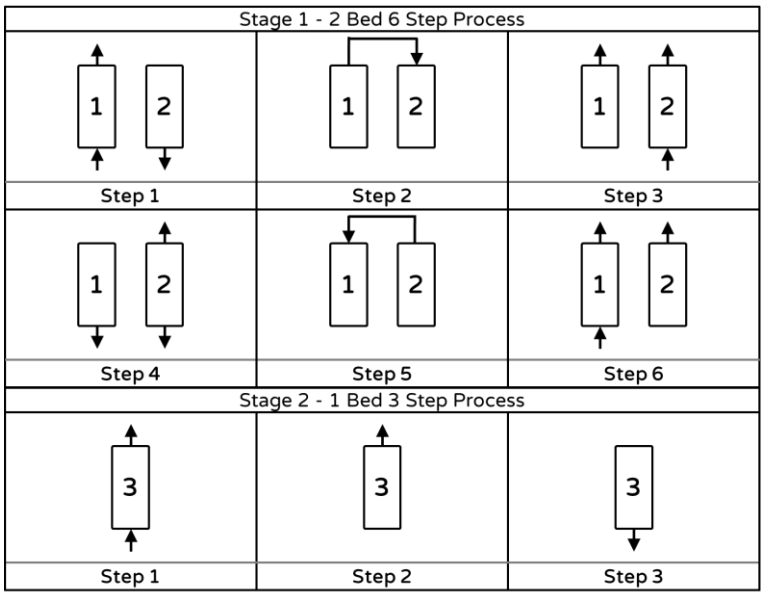


Figure 8: Schematic Diagram of the VPSA Two-Stage Dual-Bed Six-Step and Single-Bed Three-Step Operation Processes (Graphed in PowerPoint by TPRI)

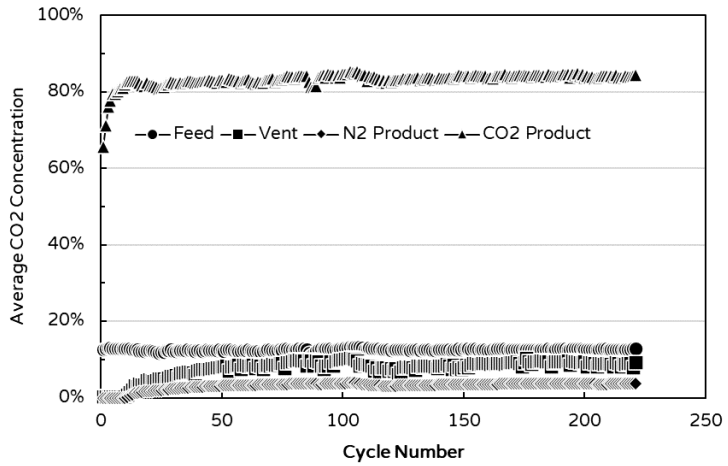


Figure 9: Average $CO_2$ Concentration for Each Cycle in the First Stage of VPSA Two-Stage Process (Graphed in Excel by TPRI)

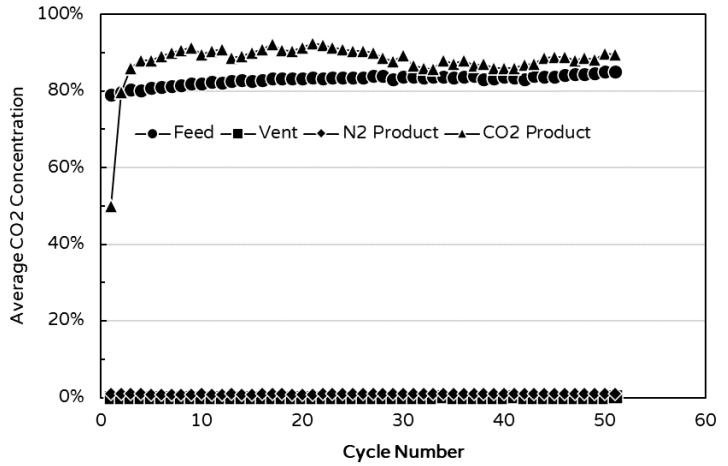


Figure 10: Average $CO_2$ Concentration for Each Cycle in the Second Stage of VPSA Two-Stage Process (Graphed in Excel by TPRI)

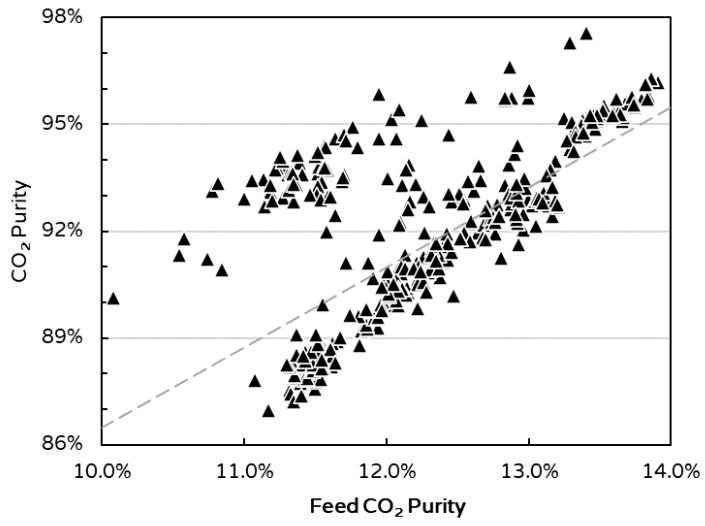


Figure 11: Scatter Plot of Post-Separation $CO_2$ Concentration to $CO_2$ Feed Concentration (Graphed in Excel by TPRI)